

Collective effects in a random-site electric dipole system: $\text{KTaO}_3\text{:Li}$

J. J. van der Klink and D. Rytz

Institut de Physique Expérimentale, Swiss Federal Institute of Technology, CH-1015 Lausanne, Switzerland

F. Borsa

*Istituto di Fisica dell'Università e Unità Gruppo Nazionale di Struttura della Materia
del Consiglio Nazionale delle Ricerche, I-27100 Pavia, Italy*

U. T. Höchli*

IBM Zurich Research Laboratory, CH-8803 Rüschlikon, Switzerland

(Received 10 June 1982)

Li, substituting for K in KTaO_3 , creates a local electric dipole, due to its off-center position with respect to the cubic site. We have studied such crystals with different amounts of Li (and in a few cases also doped with Nb, substituting for Ta) by nuclear magnetic resonance, dielectric relaxation, pyroelectricity, ultrasound, and birefringence methods. Birefringence and dielectric susceptibility results show that collective effects between the Li dipoles occur below a fairly well-defined concentration-dependent temperature of the order of 50 K, but nuclear magnetic and dielectric relaxation indicate the absence of criticality at the onset of these effects. These collective effects are related to those arising in spin-glasses. We discuss the data in the light of theoretical models and computer simulations of systems of randomly interacting moments, which predict an apparent condensation into a system of metastable clusters without long-range order.

I. INTRODUCTION

Enormous efforts have very recently been devoted towards understanding the condensed phase of randomly interacting moments. Most of the experimental reports are concerned with investigations on spin-glasses. These¹⁻¹⁹ are crystalline, often metallic substances like CuMn in which the less abundant component, Mn, carries a magnetic moment, while the other component, forming the host lattice, is magnetically inert. Spin-glasses have their electrical^{20,21} and elastic^{22,23} analogs: A dielectric lattice such as KCl may contain dipolar ions,²⁴ like OH substituting for Cl. In KTaO_3 hosting Li at K sites, the dipoles are created by the Li occupying an off-center site²⁵ near the ideal cubic K position. Interaction between the magnetic moments as in spin-glasses or electric moments as in dipole glasses gives rise to collective effects only distantly analogous to ferromagnetic and ferroelectric condensation.²⁶ The analogy between a dipole glass and a ferroelectric includes the existence of a maximum of the susceptibility at a temperature T_g coincident with the stability limit for remanent polarization, but it breaks down conspicuously for zero-field cooled samples: A spontaneous polarization is found only for periodic-array dipoles, whereas random-site dipoles condense in a way avoiding long-range correlation,¹

and a zero-field cooled configuration cannot be converted into a poled configuration by applying an electric field.

The inability of a random-site dipolar system to achieve long-range order is related to the concept of frustration,²⁷ put forward for spin-glasses. There the centrosymmetric Ruderman-Kittel-Kasuya-Yosida (RKKY) interaction²⁸ changes sign with distance. A spin surrounded by other spins at random distances may not "know" which is its appropriate state of lowest energy, and thus may be frustrated. A system which allows energetically unfavorable configurations to be (meta)stable²⁹ is nonergodic.³⁰ Near-degenerate spin configurations are thought to arise because of the lack of positive definiteness of the potential. The dipolar interaction has a similar property: It changes sign, not with distance, but with relative orientation of the moments. Its relatively complicated form seems to have deterred theoreticians from adopting the dipolar model for lattice-dynamical calculations. From an experimental point of view, however, electric-dipolar systems present some advantages: Dielectric measurements can be made with great ease and precision; the fact that samples are transparent allows for Raman^{25,31-33} and birefringence³²⁻³⁵ measurements; the strong quadrupole-strain interaction leads to "critical" ultrasonic attenuation³⁶ and dispersion,

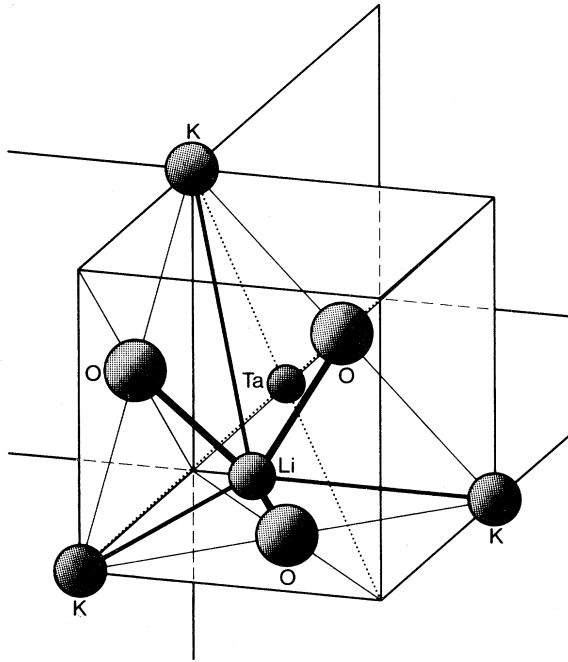


FIG. 1. Portion of the structure and Li site in $\text{KTaO}_3:\text{Li}$. Nearest neighbors of Li shown only.

and the dipoles may be chosen to carry a strong nuclear magnetic moment (as, e.g., in ^7Li), suitable for local-field investigation.³⁷

It is the purpose of this paper to present the experimental situation for random-site dipoles in $\text{KTaO}_3:\text{Li}$ and to discuss it in terms of recently advanced theoretical concepts.¹⁻¹⁹ Some of the experimental results are known from earlier work, in particular^{25,31,32} by Yacoby, who discovered the dipolar character of Li in KTaO_3 and found evidence for dipolar relaxation. It is complemented here by measurements of NMR, dielectric relaxation, pyroelectricity, birefringence, and ultrasound for samples containing Li, and in part also Nb, in different concentrations.

The off-center displacement of the Li ions at the K site is in the $[100]$ direction,³⁸ i.e., towards the center of mass of four oxygen ligands situated at $\langle 111 \rangle$ directions (Fig. 1). The amount of displacement is estimated³⁹ to be $\delta=0.9$ Å from a point-charge model for the electric field gradient (efg) measured by NMR. The cubic symmetry of the host crystal allows for six equivalent Li displacements among which transitions occur by thermal excitation. The barrier was found³⁸ to be $E_B=86$ meV ≈ 1000 K, suggesting that quantum-mechanical tunneling is negligible. The polarization P associated with each Li exceeds that arising from its own displacement.⁴⁰ As noted by Kirkwood,⁴¹ the effectively measurable polarization of an impurity

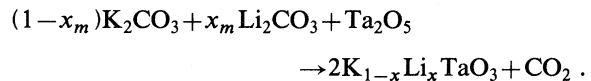
includes that induced in the lattice, and also the dynamic polarizability is enhanced by that part of the lattice which follows the motion of the impurity adiabatically. The enhancement factor, which is a measure for the correlation volume, is a property of the host lattice and does *not* depend upon correlation between Li-dipole orientations. We note here a limited analogy with $\text{KCl}:\text{OH}$ where the OH dipole tunnels²⁰ between equivalent $\langle 100 \rangle$ directions, the barrier height being ~ 0.8 meV. The weak lattice polarizability of KCl limits enhancement effects, and reduced screening of dipolar interaction puts the limiting concentration for single-ion behavior²⁰ to 4×10^{-5} . At higher concentrations collective effects are seen around 1 K. KTaO_3 has a particularly large dielectric susceptibility arising from the strongly anisotropic oxygen polarizability.⁴² This screens dipolar interaction effectively⁴³ so that concentrations above one percent are required for noticeable interactions between Li dipoles. Collective effects occur in a temperature range around 50 K. The more convenient temperature range and the larger concentrations with concomitant large sensitivities certainly favor experimental investigations.

The experimental results will be presented in some detail in Sec. II. They are summarized in Sec. III, showing the physical picture emerging from the data obtained by six different methods. Also in Sec. III theoretical models are reviewed which aim at explaining randomly interacting (mostly magnetic) moments. They are much simpler than the experimental situation requires, but some of their predictions are experimentally confirmed. Finally, in the conclusion we briefly consider the controversy^{33,34,38} over the nature of the collective effects in $\text{KTaO}_3:\text{Li}$, and argue that they are more similar to those in spin-glasses than to those in other perovskite ferroelectrics.

II. EXPERIMENTAL RESULTS

A. Sample preparation

All the samples were obtained by spontaneous nucleation in high-temperature solutions⁴⁴:



Details on the slow-cooling method employed and on determination of the Li concentration x may be found elsewhere.⁴⁵ The values of x quoted in the present work are those obtained from direct NMR calibrations where available, and interpolated with $x=0.35x_m$ in other cases.⁴⁵ This latter relation had been used for all samples in Ref. 38, which explains

some slight differences in x values. The present values are some 15% lower than the estimated values given in Ref. 40. For the doubly-doped (Li and Nb) species, no analysis was made, and the concentrations quoted are those of the ingot scaled to the best of our experience.

From birefringence observations, to be discussed in Sec. IIF, we find the transition temperature as function of x to be given by $T_g = 535x^{0.66}$ K. To within the stated error limits (typically several degrees) the data given by other authors^{32,33} agree well with this expression, as shown in Fig. 2. The agreement is somewhat surprising, since the concentration scale used by Prater *et al.*³³ probably corresponds to our x_m , whereas Yacoby does not give details on the scale he used.³²

B. Nuclear magnetic resonance and relaxation

1. Static properties of Li nuclei

The quadrupole moment of the ^7Li nucleus is used here as a local probe to obtain insight into the static and dynamic phenomena accompanying the freezing process. The static and time-dependent

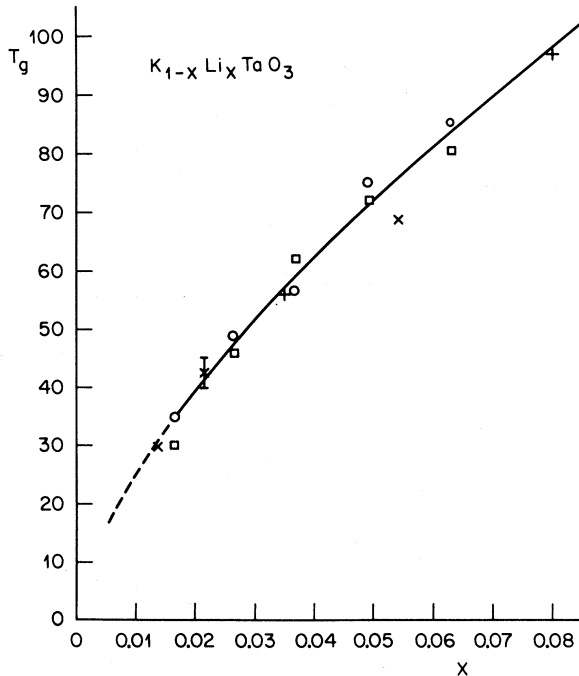


FIG. 2. Freezing temperature T_g vs concentration in $\text{KTaO}_3:\text{Li}$ from different researches. Circles and squares are our results from birefringence (Δn) and from the maximum in the dielectric susceptibility ($\Delta\epsilon$). The pluses are from Ref. 32 and the crosses from Ref. 33. The solid line is fit to our birefringence data, yielding $T_g = 535x^{0.66}$ K.

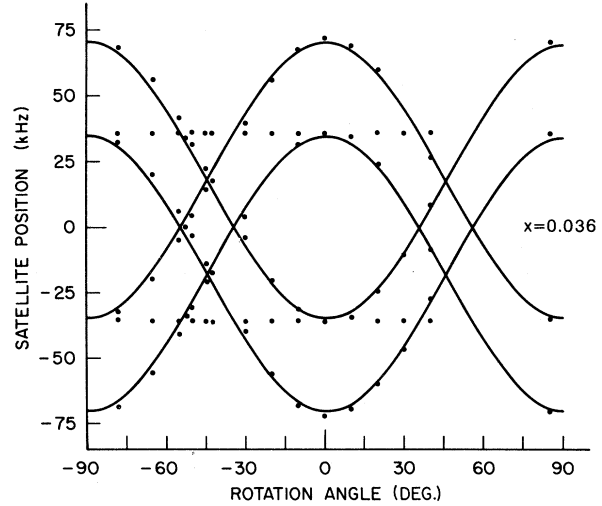


FIG. 3. Fit of the satellite lines to Eq. (1) for a determination of the quadrupole splitting $\nu_Q = 70$ kHz, $x = 0.036$. Note that one pair of satellites does not shift with rotation around a cubic axis.

perturbation of the Zeeman Hamiltonian due to coupling of the quadrupole moment with the electric field gradient tensor is investigated to obtain information about the local crystal symmetry at the average position of the ^7Li nucleus and about the dynamics of the ^7Li ion.

The shape of the ^7Li NMR spectrum was obtained by Fourier transform of the free-precession decay following a $\pi/2$ rf pulse. The measurements were performed at 21, 26.5, and 32 MHz with a typical rf field intensity $H_1 \sim 30$ G.

At low temperature, a NMR spectrum split by first-order quadrupole interaction is observed. The position of the quadrupole satellites as a function of the orientation of the magnetic field H_0 in the (100) plane is shown in Fig. 3 and can be described by

$$\nu_{\pm} = \nu_L \pm \nu_Q (3 \cos^2 \theta - 1) / 2, \quad (1)$$

where ν_L is the Larmor frequency and $\nu_Q = e^2 q Q / 2h$ the quadrupole-coupling frequency for $I = \frac{3}{2}$. Equation (1) holds for an axially symmetric electric field gradient with maximum component eq along the z axis and where θ is the angle between H_0 and the z axis.

Extremum positions of the satellites are found for $H_0 || [010]$ and $H_0 || [001]$. Also when $H_0 || [111]$, the quadrupole splitting vanishes. This rotation pattern allows one to conclude unambiguously that at low temperature, the Li occupies sites of locally uniaxial symmetry along [100]. Furthermore, the ratio of the intensity of the quadrupole satellites at different angles is consistent with an approximately (but perhaps not exactly) equal probability for the sym-

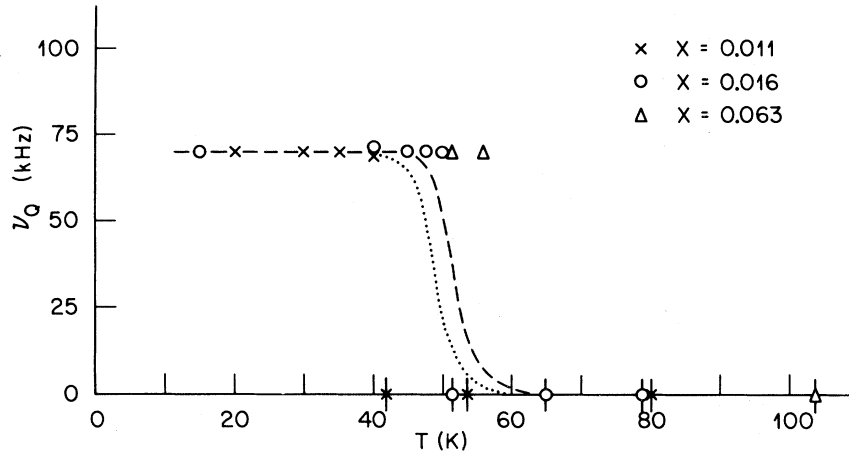


FIG. 4. Temperature dependence of quadrupole splitting in KTaO_3 . The signatures of the data denote samples with different concentration. The theoretical behaviors predicted by Eq. (9) are indicated as the dotted line ($x=0.011$) and the dashed line ($x=0.016$).

metry axis to lie along any of the three equivalent $\langle 100 \rangle$ directions. The observed quadrupole-coupling frequency is independent of temperature and Li concentration.

A transition from a quadrupole-split spectrum to a single-line spectrum takes place in a temperature interval of less than five degrees around 50 K, indicating that the Li ion occupies, on the average, a site of cubic symmetry (Fig. 4). The average is on the time scale of the inverse quadrupole-coupling frequency.

To establish the size of the Li displacement, we compare the experimental value of ν_Q with the one estimated on a point-charge approximation which is known⁴⁶ to yield the correct efg in other perovskite crystals undergoing structural phase transitions. We use $Q=0.042 \times 10^{-24} \text{ cm}^2$, $(1-\gamma_\infty)=0.74$ appropriate for the Li^+ ion, $Z=+5$ for the valence of the Ta ion, and $Z=-2$, $Z=+1$ for that of the oxygen and the alkaline ion, respectively. The calculated quadrupole-coupling frequency associated with an off-center displacement δ of the Li atom, taking only nearest-neighbor contributions into account, amounts to

$$\nu_Q = 1.3 \times 10^6 \left(\frac{\delta}{a} \right)^2, \quad (2)$$

in units of Hz. From the experimental result $\nu_Q=70 \text{ kHz}$, and $a=4 \text{ \AA}$, we conclude that the displacement is $\delta=0.9 \text{ \AA}$.³⁹ A similar calculation for a hypothetical tetragonal distortion of the unit cell, without off-center displacement of the Li, up to the sixth nearest neighbor yields

$$\nu_Q = -1.05 \times 10^5 (a^3/c^3 - 1) + 3.5 \times 10^5 (a^2/c^2 - 1) \quad (3)$$

(in units of Hz). For a value of $c/a=1.01$, typical of the ferroelectric perovskite-type crystals,⁴⁷ Eq. (3) yields $\nu_Q=10 \text{ kHz}$ which is too small to explain the observed quadrupole-coupling frequency. Still, the occurrence of a ferroelectric-type transition with such a tetragonal distortion of the cell should not remain undetected in NMR experiments since the expected quadrupole splitting of 10 kHz exceeds the observed dipolar linewidth of 3 kHz. Intercell contributions to the efg due to the interaction of a ^7Li nucleus with the electric dipole moment associated with the off-center displacement of the Li atoms in a different cell turn out to be negligible. These contributions are of the order of $V_{zz} \sim 6\mu/a^4$, where μ is the effective electric dipole moment and a is the average Li-Li distance, $a \sim a(x^{-1/3})$. For $x=0.02$ and $\mu=5 \times 10^{-17} \text{ esu}$, corresponding to the moment enhanced by polarization effects,⁴⁰ one finds $\nu_Q^{IC}=1.8 \text{ kHz} \ll \nu_Q^{\text{expt}}$. Evidence is thus compelling to conclude that the observed quadrupole coupling is related to the gradual freezing of the Li in an off-center position and that no significant ($c/a \geq 1.01$) tetragonal distortion of the unit cell occurs.

2. Spin-lattice relaxation and dynamic properties of ^7Li nuclei

The nuclear spin-lattice relaxation rate was measured by monitoring the return to the equilibrium value of the nuclear magnetization following a $(\pi/2)_x - (\pi/2)_x$ pulse sequence. When no static quadrupole effects are present, recovery of the nuclear magnetization should be exponential if a common spin temperature among the Zeeman levels is maintained during the relaxation process.⁴⁸

In contrast to the expectation, in a temperature range of about 100 K above the temperature at

which static quadrupole effects appear, the recovery is strongly nonexponential for certain orientations of the crystal with respect to the external magnetic field. But for some particular crystal orientations, we have obtained exponential recovery curves at all temperatures investigated and our quantitative discussion will be restricted to these results. The temperature dependence of the relaxation rate is indicative of fluctuations of the efg tensor driven by a thermally activated hopping motion.^{38,49} In the weak-collision approach and for $I = \frac{3}{2}$, one can write for the relaxation transition probabilities⁴⁸

$$W_1 = \frac{1}{12} \left[\frac{eQ}{\hbar} \right]^2 \int_{-\infty}^{-\infty} \langle V_1(0)V_{-1}(t) \rangle \times \exp(i\omega_L t) dt, \quad (4)$$

$$W_2 = \frac{1}{12} \left[\frac{eQ}{\hbar} \right]^2 \int_{-\infty}^{-\infty} \langle V_2(0)V_{-2}(t) \rangle \times \exp(i2\omega_L t) dt,$$

from $\Delta m = \pm 1$ and ± 2 , respectively. The efg tensor components are calculated in the local principal frame of reference, and the time dependence of the perturbation arises from the change of relative orientation of the efg principal axes with respect to the external magnetic field as the Li atoms perform jumps through 90° among the six equivalent off-center positions along the $\langle 100 \rangle$ directions. Jumps through 180° do not modulate the efg tensor and can be neglected for the spin-lattice relaxation process. For the correlation function, we assume an exponential decay with its correlation time τ_c given by an Arrhenius law. For the magnetic field in the (100) plane at angle β with one of the cubic axes and for

an isotropic hopping of the Li, we find

$$W_1 = 4\pi^2 \langle v_Q^2 \rangle \frac{\tau_c}{1 + \omega^2 \tau_c^2} \sin^2 \beta \cos^2 \beta, \quad (5)$$

$$W_2 = \pi^2 \langle v_Q^2 \rangle \frac{\tau_c}{1 + 4\omega^2 \tau_c^2} (1 - \sin^2 \beta \cos^2 \beta).$$

If energy-conserving transitions among the Zeeman levels are assumed to be frequent enough to ensure a common spin temperature during the relaxation process, it follows that recovery is exponential for all orientations and⁴⁸

$$T_1^{-1} = (2W_1 + 8W_2)/5. \quad (6)$$

In the opposite limit of no energy exchange among the Zeeman levels, solution of the master equations yields for the recovery law⁵⁰

$$\frac{M(t) - M(\infty)}{M(\infty)} = -\frac{1}{5} \exp(-2W_1 t) - \frac{4}{5} \exp(-2W_2 t), \quad (7)$$

which is, in general, nonexponential.

At high temperatures, such that $\omega\tau \ll 1$, one finds from Eqs. (5) that $W_1 = W_2$ for the particular orientation $\beta = 31.7^\circ$, and Eq. (7) predicts an exponential decay with

$$\frac{1}{T_1} = \frac{8}{5} \pi^2 \langle v_Q^2 \rangle \tau_0 \exp \left[\frac{E_B}{kT} \right], \quad (8)$$

where E_B is the height of the barrier to reorientation of the Li-induced dipole.

The experimental values can be fitted very well by Eq. (8) as we have shown earlier.³⁸ Fitting to Eq. (8) the T_1^{-1} vs T data from Ref. 38 over the whole temperature range reported yields the parameter values given in Table I.

TABLE I. Values of the parameters describing the Li dynamics as obtained by different methods. Note the good agreement between the two determinations of T_g , and their relation to T_{thaw} . Note also that T_Q describes the transition in Fig. 4, and is *not* related to T_g .

	Method	Eq.	Li concentration x				Units
			0.011	0.016	0.026	0.063	
E_B	NMR	(8)	1000	1090	850	980	K
E_B	dielectric		1000	1100	1100		K
τ_0	NMR	(8)	1.4	0.75	6	3.7	10^{-14} s
τ_0	dielectric		6	6	6		10^{-14} s
T_Q	spectrum	(9)	40	50		55	K
v_Q	spectrum	(1)	70	70	70	70	kHz
$\langle v_Q^2 \rangle^{1/2}$	relaxation	(8)	71	81	68	56	kHz
T_g	birefringence		< 10	35	49	85	K
T_g	dielectric		< 10	30	46	~80	K
T_{thaw}	pyroelectric		30	40	55	84	K

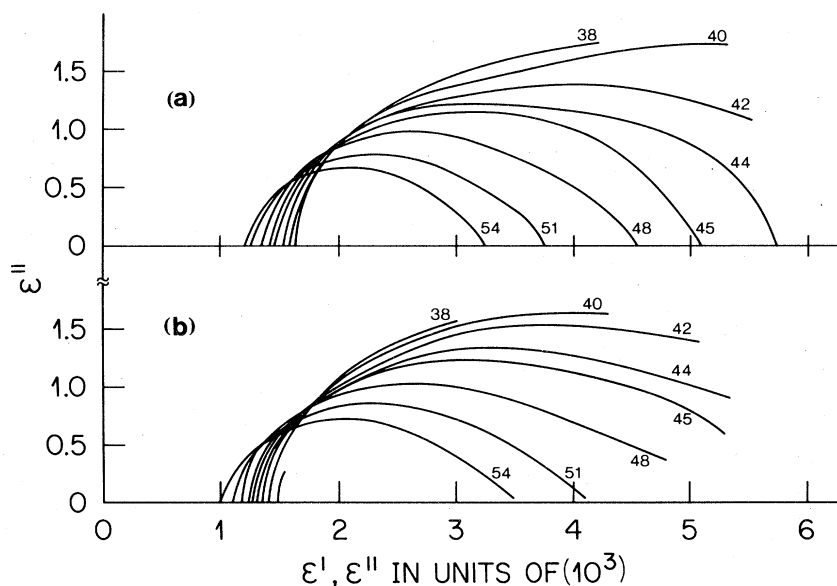


FIG. 5. Cole-Cole plots for $\text{KTaO}_3\text{:Li}$. (a) $\vec{E} \parallel [100]$ and (b) $\vec{E} \parallel [111]$. $x=0.016$.

The jumping of Li which modulates the efg and thus drives the spin-lattice relaxation takes place among the sites that give rise to the quadrupole-split spectrum. This identification not only rests on symmetry arguments but also on the good agreement between the static quadrupole constant ν_Q and its mean-square value deduced from relaxation measurements (see Table I). Appearance of the static quadrupole effects at low temperature is thus associated with the slowing down of the hopping rate to a value less than ν_Q . This can be seen by comparing

the experimental values of ν_Q vs T with the temperature dependence given by the "line-narrowing" theory of Kubo and Tomita,⁵¹ shown in Fig. 4:

$$\nu_Q^2(T) = \nu_Q^2(0) \frac{2}{\pi} \tan^{-1}[\nu_Q(T)\tau_c], \quad (9)$$

where for τ_c we use the value and the temperature dependence deduced from T_1 measurements (see Table I). The agreement is good particularly at low Li concentration. It should be noted that the apparent sharpness of transition between static and

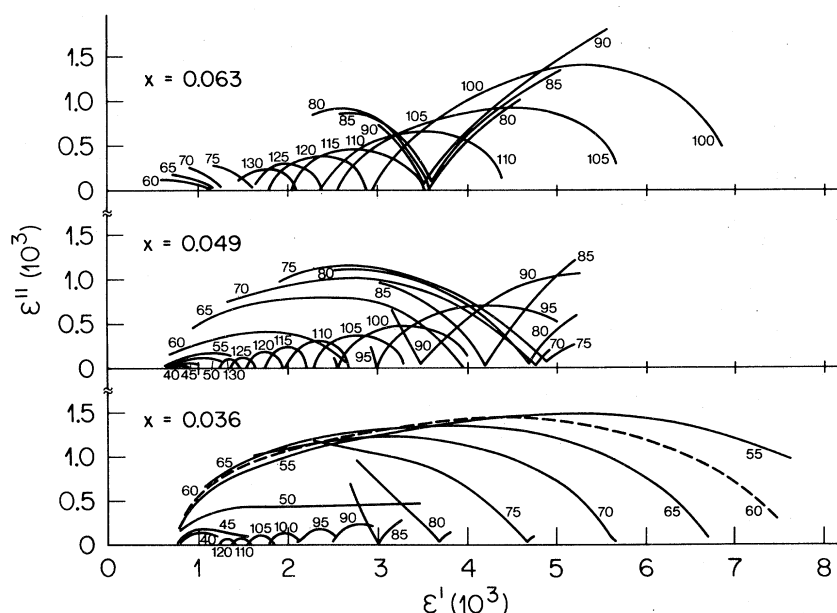


FIG. 6. Cole-Cole plot of the dielectric susceptibility in $\text{K}_{1-x}\text{Li}_x\text{TaO}_3$ vs temperature. x is labeled in the figure.

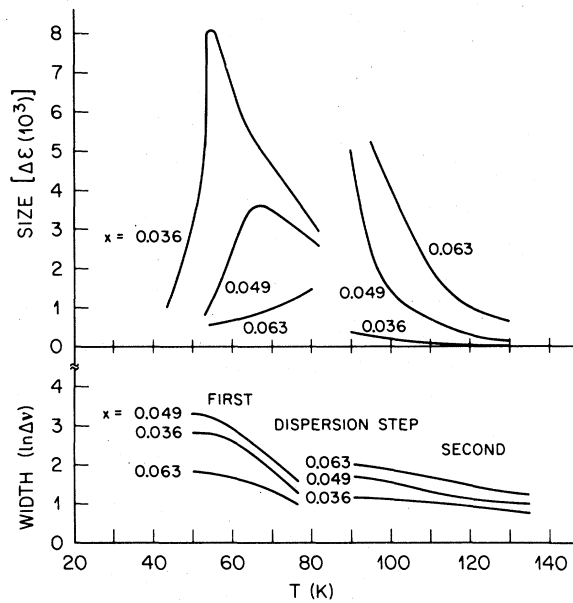


FIG. 7. Size and width of dielectric relaxation step in $K_{1-x}Li_xTaO_3$ vs temperature. Note two distinct steps, one for high T , one for low T . x labels the concentration of Li.

dynamic quadrupole coupling is largely due to the difficulties in detecting the quadrupole satellites in the "line-narrowing" region.

C. Dielectric relaxation

For Li concentrations below $x=0.03$, dielectric-relaxation measurements have been interpreted (Fig. 5) in terms of Arrhenius functions, and the param-

eters gained from the data, E_B and τ_0 , are consistent with those gained by NMR relaxation (see Table I). Two such plots are reproduced in Fig. 5 with the ac field applied parallel to [100] and [111], respectively. They are essentially identical if allowance is made for a slight change of concentration from one sample to the other. We note that close to T_g , a broadening of the dielectric response and a moderate deviation from Arrhenius behavior is observed which had been related to the onset of collective effects.^{38,52} These effects are particularly pronounced for large Li concentrations. In Fig. 6, we report Cole-Cole plots for the dielectric susceptibility as a function of temperature. The sample concentration decreases from top to bottom, $x=0.063$, 0.049, and 0.036. Quite unexpectedly, the dielectric relaxation changes its character as x increases. We note two dispersion regimes, the one at low temperature characterized by a broadening of the response near T_g and a maximum step size which decreases with x . These quantities, size [defined as $\Delta\epsilon = |\epsilon'(\max) - \epsilon'(\min)|$, where $\epsilon'(\max)$ and $\epsilon'(\min)$ are the maximum and minimum values ϵ' reaches as a function of frequency ν], and width [defined as $\Delta\nu = \nu(\max) - \nu(\min)$, where $\nu(\max)$ and $\nu(\min)$ are the frequencies for which $\epsilon' = \epsilon'(\max)$ and $\epsilon' = \epsilon'(\min)$, respectively] of the step are plotted in Fig. 7 as a function of temperature for the same samples. The second dispersion step observed at high temperature and concentration is due to a slower relaxation process than the first step. Its characteristic parameters are also plotted in Fig. 7. Its step size increases more than linearly with con-

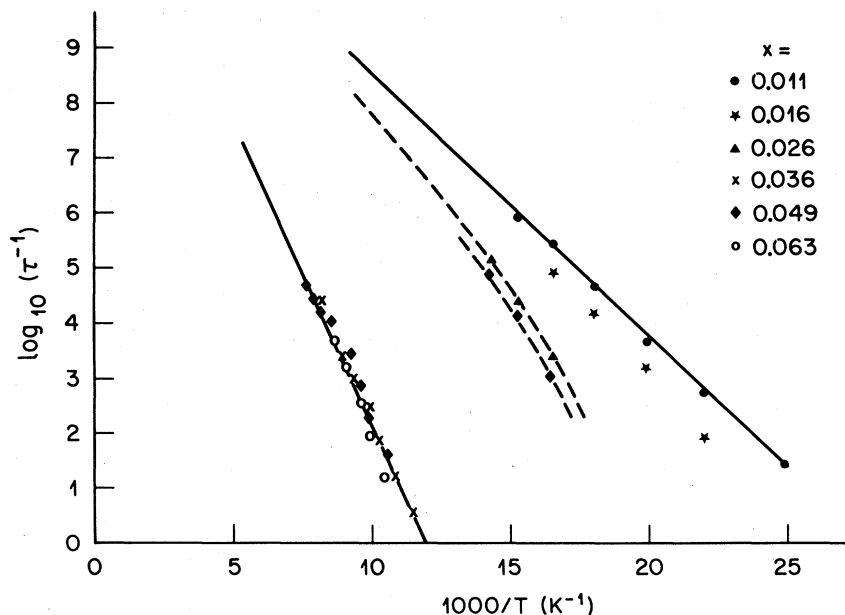


FIG. 8. Arrhenius plot of dielectric relaxation in $K_{1-x}Li_xTaO_3$. The slope of the curve gives E_B . See also Table I.

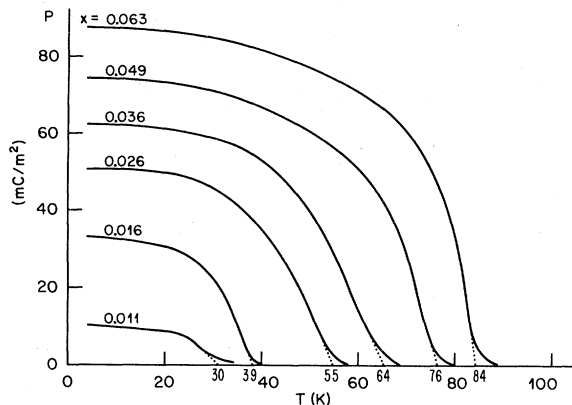


FIG. 9. Remanent polarization and the thawing temperature in $K_{1-x}Li_xTaO_3$.

centration of Li impurities, but the width changes only moderately. The most probable relaxation rate is plotted versus $1/T$ on logarithmic scale for both dispersion steps in Fig. 8. On increasing x from 0.006 to 0.026, one finds the slope of these curves to vary little except for some bending close to T_g . The parameters E_B and τ_0 are listed in Table I. At $x \geq 0.036$, both dielectric dispersion steps are visible (see Figs. 6 and 7) and an analysis similar to the one done for the upper branch in Fig. 8 yields for the lower branch a well-defined barrier of 2500 K which does not vary on further increasing x .

Dielectric relaxation has also been observed for Li dipoles in a lattice whose susceptibility was increased by the addition⁵³ of Nb ions substituting for Ta. There is a clear enhancement of the Li polarizability about in proportion to the lattice polarizability of $KTaO_3:Nb$ in the appropriate temperature range.

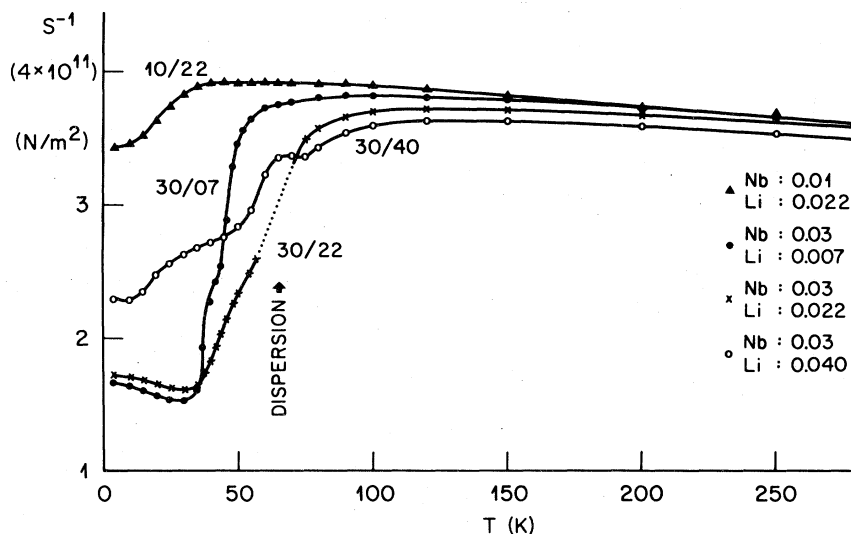


FIG. 10. Elastic compliance of $KTaO_3$ doped with both Li and Nb as a function of temperature.

D. Pyroelectric effect

Upon cooling with an electric field applied, a polarization can be induced which remains when the field is turned off at low T . It is not possible to induce a polarization on a sample which has been cooled at zero field. The remanent field was measured by its pyroelectric current stored as charge in an electrometer while the sample was slowly heated from 4 K through to T_g . The results are shown in Fig. 9. Clearly, the curves $P(T)$ have an appearance similar to that of a ferroelectric, where $P \sim \sqrt{T_c - T}$, but there are two main differences. Firstly, P is a remanent polarization which cannot be measured by the hysteresis effect implemented by the time-honored Sawyer-Tower method, and secondly, P is a near-linear function of x at 4 K for $x < 0.04$ and saturates at $x > 0.04$. This is in contrast to the findings⁵² in $KTa_{1-y}Nb_yO_3$ where, at 4 K, the polarization remains zero below $y = 0.008$ before it starts rising as $y - y_c$. To determine the thawing temperature, we have ignored the tail of P vs T presuming it arises from either surface effects or the inherent failure to make a true static measurement. Thus, allowing for an uncertainty of 2 K, we are able to determine T_{thaw} and insert the values in Table I.

E. Sound propagation

The influence of polarizable Li dipoles on sound propagation was the subject of an earlier paper.⁵⁴ It was shown that the dispersion relations were the same for sound as for the dielectric response provided $x < 0.03$. The same mechanism, namely, 90° flips of Li dipoles, was held responsible for dielectric and

ultrasonic dispersion. In addition, the linear increase of the elastic compliance s with x at 4 K suggested that the condensed phase was reached by gradual freezing of polar clusters and not by a thermodynamic-type transition. Quite in contrast to this behavior is quantum ferroelectric $\text{KTa}_{1-y}\text{Nb}_y\text{O}_3$, where, at 4 K, $s(y)$ has step-function-like behavior.⁵²

Here, we present a few results on sound propagation in KTaO_3 doped with both Li and Nb: Li doping was intended to provide a relaxation mechanism for the strain, whereas Nb doping should force the sample into a ferroelectric state at finite temperature. Figure 10 shows the elastic compliance of $\text{K}_{1-x}\text{Li}_x\text{Ta}_{1-y}\text{Nb}_y\text{O}_3$ as a function of temperature. Clearly, the elastic results unify both the features of $\text{KTaO}_3\text{:Nb}$, a step function at T_c , and of $\text{KTaO}_3\text{:Li}$, a Debye relaxation function. The transition temperature T_c as deduced from the elastic step is essentially given by that of "pure" $\text{KTaO}_3\text{:Nb}$, about 20 K for 1% Nb and about 50 K for 3% Nb. On the other hand, the width of the relaxation step is proportional to the Li concentration to within the admittedly large uncertainty of the actual concentration.

F. Optical measurements

Several authors³²⁻³⁵ have confirmed and extended our observation³⁸ that $\text{KTaO}_3\text{:Li}$ crystals show birefringence below the temperature T_g at which the maximum in the dielectric constant of the Li system occurs, and that we have identified with a glass transition temperature. In fact, transition temperatures determined from birefringence by observing the whole crystal in white light, as in Ref. 35, agree well with those from dielectric results, as shown in Fig. 2. On the same figure we have plotted the transition points observed by other authors in their birefringence experiments. The transition tempera-

tures do not markedly differ from ours, but there is a wide variation in the details of the observed birefringence patterns,^{32-35,55} to which we shall refer below.

III. DISCUSSION

A. Summary of experimental results

The main features of $\text{KTaO}_3\text{:Li}$ at low concentrations of Li ions are as follows: (1) the direction and (2) the amount δ the Li is displaced with respect to the inversion-symmetric K position, (3) the total polarization P (including that of the surrounding lattice) associated with a displaced Li ion, and (4) the energy E_B needed for Li to pass from one to another 90-deg-distant equivalent position. The results gained by different methods are summarized in Tables I and II and their internal consistency is briefly discussed here.

Single Li ions are displaced in the [100] or equivalent directions as observed by NMR,³⁸ pyroelectric,⁴⁰ ultrasound,⁵⁴ and Raman^{32,33} experiments. Their displacement³⁹ is $\delta=0.9 \text{ \AA}$ as estimated from the electric field gradient in NMR measurement. This displacement is *less* than the maximum allowed by a hard-sphere cage, which means that the electronic shell of the oxygens moves towards the displaced Li. These oxygens in turn polarize the lattice further away from the Li.

The total polarization measured in dielectric⁵⁶ and pyroelectric⁴⁰ experiments thus exceeds that of the Li given by $P_{\text{Li}}=m_{\text{Li}}e\delta$, where m_{Li} is the number of Li/m³. We consider the enhancement factor of ~ 10 to be a measure of the correlation volume. For $x \gg 0.04$ the polarization is no longer proportional to the Li content but saturates at a value of $\sim 150 \text{ mC/m}^2$. Attempts to switch or "turn on" the polarization below T_g fail as evident from birefringence,³⁵ pyroelectric,⁴⁰ and ultrasound measurements.⁵⁴ This

TABLE II. Properties of Li dipoles in KTaO_3 and the experimental methods by which they have been studied. The last line refers to the sections in which the various experiments are discussed in detail.

	NMR	Dielectric	Pyroelectric	Ultrasound	Birefringence	Raman
Site symmetry	×			×		×
Bare dipole	×					
Total dipole		×	×		×	
Elastic quadrupole				×		
Transition temperature		×	×		×	
Barrier height	×	×		×		
Barrier distribution ($0.01 < x < 0.03$)		×				
Double barrier ($x > 0.03$)		×				
Section	II B	II C	II D	II E		

means that random-site dipoles cannot be switched as can periodic-site dipoles. The reason for the apparent stability of a dipolar cluster under an adverse field is the breakdown of strain-compatibility relations as required for domain-wall motion.⁵⁷

The dynamics of these Li dipoles are probed by nuclear magnetic relaxation, dielectric relaxation, and ultrasonic absorption. They are described by thermally excited jumps through 90° between equivalent positions at a rate $\tau^{-1} = \tau_0^{-1} \exp(-E/kT)$, where $\tau_0^{-1} \sim 10^{13 \pm 1} \text{ s}^{-1}$, $E = 1000 \pm 100 \text{ K} = 86 \text{ meV}$ (see Table I). Near T_g , deviations were found from the Arrhenius behavior for dielectric relaxation, but none were noticed in nuclear magnetic relaxation. In the same temperature range, according to dielectric relaxation data, the hopping time has a wide distribution of probability, just as was postulated for spin-glasses.⁵⁸ At concentrations above $x=0.03$, the distribution of dielectric relaxation times is doubly peaked with the new peak corresponding to an energy barrier of $\sim 2500 \text{ K}$ which gradually takes over all the intensity as x increases.

There are striking analogies between collective effects of $\text{KTaO}_3\text{:Li}$ and those of spin-glasses. These analogies are a cusp of the susceptibility at a concentration-dependent temperature $T_g(x)$,³⁸ and a remanent polarization with a stability limit near $T_g(x)$, where for $x > 0.01$ $T_g(x) \sim x^{0.66}$ is a monotonous function of x . The freezing temperature is associated with the onset of birefringence. The spatial distribution of light intensity observed in birefringence measurements by different authors^{32-35,55} appears to vary considerably. In particular, full birefringence oscillations have been observed by Courtens in a selected spot of his crystal by discarding somewhat arbitrarily the information obtained from the much more abundant structured regions. He states that homogeneous domains exist of the order of $100 \mu\text{m}$ or more. This is at variance with other observations⁴¹ and also at variance with the conclusions by Prater *et al.* drawn from Raman-scattering measurements.³³

The phase diagram (see Fig. 2) shows that (for $x > 0.01$) T_g increases less than linearly with x and the transition line is well described by $T_g = 535x^{0.66}$. This power law may be significant: Mean-random-field (MRF) calculations⁵⁹ predict $T_g \propto x^\alpha$ with $0.5 < \alpha < 1.0$. Similar power laws have been observed in spin-glasses,¹ whereas for purely structural phase transitions⁴⁹ in mixed perovskite $\text{K}_{1-c}\text{Rb}_c\text{MnF}_3$ and antiferroites $[\text{K}_{1-c}(\text{NH}_3)_c]_2\text{SnCl}_6$, where a phase transition is observed for $c=0$ and none for $c=1$, the shift of the transition temperature is linear in c for small concentrations. In $\text{KTa}_{1-y}\text{Nb}_y\text{O}_3$, for y sufficiently high to be out of

the quantum limit, the transition temperature also increases linearly with y .⁵² For a crystal with $x=0.011$, where Fig. 2 predicts $T_g \approx 25 \text{ K}$, we have not observed a transition down to around 10 K . The MRF model predicts that a minimum x is necessary for ordering to occur.

B. Theories

The theoretical approach which comes closest to describing the phenomena observed in $\text{KTaO}_3\text{:Li}$ is by Fischer and Klein⁵⁹ and was intended to account for collective effects in KCl:OH .^{20,21,24} It is based on the assumption that the field acting on the dipole is given by the average random field gained from the probability distribution.⁶⁰ It is found that the susceptibility cusps at a concentration-dependent temperature, as confirmed by experiment.³⁸ A broadening of the field distribution, predicted to occur on lowering T through T_g , could be the cause for the experimentally observed distribution of dielectric relaxation times.

What is outside Fischer and Klein's scope are dynamical effects. These have been shown to lead in magnetic systems to a condensation of a kind^{61,62} differing from thermodynamic phase transitions as envisaged by the mean-random-field theory, which, like any mean-field theory, implies ergodicity. Computer simulation studies¹⁷ on very finite systems have brought the recognition that freezing is a dynamical effect in which slow and large clusters grow to become slower and larger until their dynamics turn into an apparently static disordered configuration on all experimental time scales. However, these simulations are generally made for spin-glasses, i.e., postulating centrosymmetric RKKY forces between magnetic moments. It is interesting that in these simulations, collective effects are obtained only after introducing an anisotropic perturbation.^{16,18,19}

A complication does arise for dipoles. The polarizable lattice reduces the interaction about in proportion to ϵ_l . On the other hand, it attributes to the impurity dipole a poled lattice portion⁴¹ which, in the case of KTaO_3 , exceeds the impurity polarization by 1 order of magnitude at least, but very much less⁶³ in KCl . These enhancement factors are poorly known,^{64,65} and even a quite reliable estimate of their magnitude⁶⁶ (as exists in KTaO_3) is insufficient information for a modification of the interaction potential because it obviously depends on the *shape* of the correlation volume.

The question was addressed⁶⁷ as to the possibility of a transition to a long-range polar order, if the correlation length of the host lattice exceeds the

average distance between impurities. It has been pointed out that the dipolar interaction is modified in a polarizable host lattice.⁶⁷

C. Conclusions

The large body of experimental results in $\text{KTaO}_3\text{:Li}$ collected in different laboratories and with different techniques provides clear evidence for collective effects associated to Li dipoles. The nature of the condensed state occurring below a certain temperature has been considered in analogy to spin-glass states by some authors and in terms of ferroelectricity by others. Notably the observation of birefringence has been considered an indication of ferroelectricity, with estimates of domain sizes by different authors varying between ~ 0.1 and ≥ 100 μm . The observation of a region of homogeneous birefringence does not imply, however, that the region is monodomain³²: 180° jumps of polarization go undetected in a birefringence experiment. A similar argument has been given to explain the apparently contradictory results from birefringence and Raman measurements on doubly-doped crystals.⁵⁵ As further support for this idea, we note that the electric field generated by a homogeneous polarization is $P/\epsilon\epsilon_0 \sim 10^7$ V/m amounting to a voltage of 3 kV across a 300- μm spot. This cannot possibly be compensated by the few scarce other regions which exist between the electrodes, and should, consequently, lead to a large voltage across the electrodes. However, such voltages are not observed and, in addition, birefringence patterns do not depend on open or short-circuit conditions of the electrodes.

Even in a typical ferroelectric the polarization is not homogeneous, but is broken up into domains, typically of (10–100)- μm size, due to depolarization effects. In the case of $\text{KTaO}_3\text{:Li}$, the homogeneous spots in birefringence put an upper limit of 4000 \AA (in an exceptional case > 100 μm) on the domain size while Raman scattering sets this limit far below the wavelength of light. Since, in addition, these regions of nonzero polarization appear to be insensitive to electric fields at $T < T_g$, their origin is very unlikely due to depolarization effects. The phenomenon is, however, reminiscent of remanent magnetization in a spin-glass.

The most important single argument against the occurrence of a ferroelectric phase transition is the total absence of any critical effects in the dynamics, as measured by dielectric and NMR relaxation. At such a transition, be it of displacive or of order-disorder type, a critical contribution to the spin-lattice relaxation⁴⁶ $T_1^{-1} \propto (T - T_c)^n$ and a single excitation dielectric relaxation step, or alternatively a

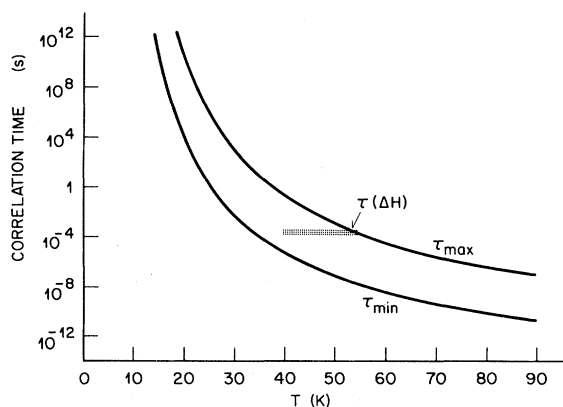


FIG. 11. Correlation time τ_c as a function of temperature for the Li hopping from T_1 (solid lines for minimum and maximum) and from the spread ΔH of the spectrum (cross hatched).

Curie-Weiss law, are predicted. None of these phenomena is found in $\text{KTaO}_3\text{:Li}$, but a smooth slowing down of the Li dynamics with temperature is observed. In Fig. 11 we show the bounds for τ_c [see Eq. (5)] derived from our NMR results,³⁸ as a function of temperature. Also indicated is the temperature region where the quadrupole structures disappear, and the corresponding range of τ_c values that has been used in the calculation [see Eq. (9)]. It is seen that both determinations of the value of τ_c in the temperature range around 50 K agree well. At lower temperatures, specific-heat data show⁶⁸ dynamic effects in the millihertz range around 30 K, in order-of-magnitude agreement with the values in Fig. 11. So, if we rely on this estimate for τ_c , we may conclude that below 20 K almost any experiment will find the system *static* in nature, independent of x . The plots in Fig. 11 are based on the assumption of a single correlation time, whereas dielectric results show a broad distribution (a T_1^{-1} vs T plot is not very sensitive to most distributions). From the absence of observable quadrupole satellites however, we estimate that for the sample with $x=0.049$ at the transition temperature, at least half of the Li jump at rates of the order 10^4 s^{-1} or faster. This is in line with the observation of pretransition clusters in the order-disorder KDP-type (potassium dihydrogen phosphate type) ferroelectrics fluctuating at similar rates above the transition temperatures.⁶⁹

The arguments in favor of a dipole-glass type of transition are mainly derived from analogies with experimental results on spin-glasses: (i) the absence of a spontaneous macroscopic polarization below T_g , (ii) the occurrence of thermoremanent polarization, (iii) the existence of a frequency-dependent maximum of the dielectric response function around

T_g , and (iv) the T_g vs x relationship is of the type $T_g \propto x^\alpha$ where $\alpha < 1$. The phase diagram and the temperature dependence of the susceptibility are in qualitative agreement with theoretical predictions for systems of random electric dipoles.⁵⁹ The absence of critical dynamics has also been found in *AuFe* and *CuMn*,⁷⁰ where, in the temperature region $0.5T_f < T < 1.2T_f$, the correlation time of the impurity moment decreases from 10^{-5} to 10^{-12} s. Thus, although a considerable slowing down occurs around T_f , the moments still fluctuate around their frozen positions at an appreciable rate, and no criticality is observed.

The strong analogy between *KTaO₃:Li* and, say, *CuMn*, suggests a common origin of their ground state. The absence of all truly critical effects in those systems suggests that the ground state of dipole glass (and of a spin-glass) is probably not ther-

modynamically different from a disordered paraelectric state but that dynamics of the collective motion become so slow that experiments always see the response of a metastable state. It is in this spirit that most recent theories treat spin-glasses and simulations of spin dynamics are made.

ACKNOWLEDGMENTS

It is our great pleasure to acknowledge numerous stimulating discussions and correspondence with J. Mydosh, A. Rigamonti, and W. N. Lawless, A. Châtelain, G. Toulouse, L. L. Chase, and L. A. Boatner. Continued technical expertise by H. E. Weibel made this research possible. We also appreciated the translation of Ref. 67 by Y. Rytz-Froidevaux.

*Present address: Istituto di Fisica dell'Università di Pavia, I-27100 Pavia, Italy.

¹J. A. Mydosh, in *Disordered Systems and Localization*, Vol. 149 of *Lecture Notes in Physics*, edited by C. Castellani and C. Di Castro (Springer, Berlin, 1981), and references therein.

²E. D. Dahlberg, M. Hardimann, R. Orbach, and J. Souletie, *Phys. Rev. Lett.* **42**, 401 (1979).

³W. Kinzel, *Phys. Rev. B* **19**, 4595 (1979).

⁴J. L. Tholence, *Solid State Commun.* **35**, 113 (1980).

⁵U. Atzmony, E. Gurewitz, M. Melamud, H. Pinto, H. Shaked, G. Gorodetsky, E. Hermon, R. M. Hornreich, S. Shtrikman, and B. Wanklyn, *Phys. Rev. Lett.* **43**, 782 (1979).

⁶R. A. Webb, G. W. Crabtree, and J. J. Vuillemin, *Phys. Rev. Lett.* **43**, 796 (1979).

⁷M. B. Salamon, K. V. Rao, and H. S. Chen, *Phys. Rev. Lett.* **44**, 596 (1980).

⁸H. M. Bolzer, C. M. Gould, and W. G. Clark, *Phys. Rev. Lett.* **45**, 1303 (1980).

⁹U. Hardebusch, W. Gerhardt, and J. S. Schilling, *Phys. Rev. Lett.* **44**, 352 (1980).

¹⁰Y. Yeshurun, M. B. Salamon, K. V. Rao, and H. S. Chen, *Phys. Rev. B* **24**, 1536 (1981).

¹¹W. E. Fogle, J. D. Boyer, N. E. Phillips, and J. Van Curen, *Phys. Rev. Lett.* **47**, 352 (1981).

¹²R. J. Birgenau, R. A. Cowley, G. Shirane, and H. J. Guggenheim, *Phys. Rev. Lett.* **37**, 940 (1976).

¹³G. Parisi and G. Toulouse, *J. Phys. (Paris) Lett* **41**, 361 (1980).

¹⁴A. J. Bray and M. A. Moore, *Phys. Rev. Lett.* **47**, 120 (1981).

¹⁵S. K. Ma, *Phys. Rev. B* **22**, 4484 (1980).

¹⁶S. E. Barnes, *Phys. Rev. Lett.* **47**, 1613 (1981).

¹⁷L. R. Walker and R. W. Walstedt, *Phys. Rev. B* **22**, 3816 (1980).

¹⁸R. W. Walstedt and L. R. Walker, *Phys. Rev. Lett.* **47**,

1627 (1981).

¹⁹P. M. Levy and A. Fert, *Phys. Rev. B* **23**, 4667 (1981).

²⁰W. Känzig, H. R. Hart, and S. Roberts, *Phys. Rev. Lett.* **13**, 543 (1964).

²¹R. Brout, *Phys. Rev. Lett.* **14**, 175 (1965); W. N. Lawless, *Phys. Kondens. Mater.* **5**, 100 (1966).

²²A. Loidl, R. Feile, and K. Knorr, *Z. Phys. B* **42**, 143 (1981); *Phys. Rev. Lett.* **48**, 1263 (1982).

²³M. Rossinelli and M. A. Bosch, *J. Phys. C* **13**, L671 (1980).

²⁴V. Narayanamurti and R. O. Pohl, *Rev. Mod. Phys.* **42**, 201 (1970).

²⁵Y. Yacoby and S. Yust, *Solid State Commun.* **15**, 715 (1974).

²⁶L. Kadanoff, L. P. Kadanoff, W. Götze, D. Hamblen, R. Hecht, E. A. S. Lewis, V. V. Palciauskas, M. Rayl, J. Swift, D. Aspnes, and J. Kane, *Rev. Mod. Phys.* **39**, 395 (1967).

²⁷M. Gabay and G. Toulouse, *Phys. Rev. Lett.* **47**, 201 (1981).

²⁸See, for example, D. Mattis, *The Theory of Magnetism* (Harper and Row, New York, 1965), p. 197.

²⁹S. A. Safran, *Phys. Rev. Lett.* **46**, 1581 (1981).

³⁰P. W. Anderson, in *Ill-Condensed Matter*, edited by R. Balian, R. Maynard, and G. Toulouse (North-Holland, Amsterdam, 1979), p. 162; A. Blandin, *J. Phys. (Paris) Colloq.* **39**, C6-1499 (1978).

³¹Y. Yacoby, W. B. Holzapfel, and D. Bäuerle, *Solid State Commun.* **23**, 947 (1977).

³²Y. Yacoby, *Z. Phys. B* **41**, 269 (1981).

³³R. L. Prater, L. L. Chase, and L. A. Boatner, *Phys. Rev. B* **23**, 5904 (1981).

³⁴E. Courtens, *J. Phys. C* **14**, L37 (1981).

³⁵P. Cornaz, U. T. Höchli, and H. E. Weibel, *Helv. Phys. Acta* **54**, 226 (1981).

³⁶N. E. Byer and H. S. Sack, *Phys. Rev. Lett.* **17**, 72 (1966).

- ³⁷D. W. Aldermann and R. M. Cotts, *Phys. Rev. B* **1**, 2870 (1970).
- ³⁸F. Borsa, U. T. Höchli, J. J. van der Klink, and D. Rytz, *Phys. Rev. Lett.* **45**, 1884 (1980).
- ³⁹From a numerical structure calculation the distance is found ~ 1.2 Å [S. N. Khanna (private communication)].
- ⁴⁰U. T. Höchli, H. E. Weibel, and L. A. Boatner, *J. Phys. C* **12**, L563 (1979).
- ⁴¹J. G. Kirkwood, *J. Chem. Phys.* **7**, 911 (1939).
- ⁴²R. Migoni, H. Bilz, and D. Bäuerle, *Phys. Rev. Lett.* **11**, 1155 (1976).
- ⁴³E. L. Pollock and B. D. Alder, *Phys. Rev. Lett.* **39**, 299 (1977).
- ⁴⁴D. Rytz, and H. J. Scheel, *J. Cryst. Growth* **59**, 468 (1982).
- ⁴⁵J. J. van der Klink and D. Rytz, *J. Cryst. Growth* **56**, 673 (1982).
- ⁴⁶F. Borsa and A. Rigamonti, in *Magnetic Resonance of Phase Transitions*, edited by F. J. Owens, H. A. Farach, and C. P. Poole (Academic, New York, 1979).
- ⁴⁷H. Megaw, *Crystal Structures: A Working Approach* (Saunders, Philadelphia, 1973).
- ⁴⁸A. Abragam, *The Principles of Nuclear Magnetism* (Oxford University Press, Oxford, 1961).
- ⁴⁹F. Borsa and J. J. van der Klink, *Ferroelectrics* **29**, 165 (1980).
- ⁵⁰P. S. Hubbard, *J. Chem. Phys.* **53**, 985 (1970).
- ⁵¹R. Kubo and J. Tomita, *J. Phys. Soc. Jpn.* **9**, 888 (1954).
- ⁵²U. T. Höchli, H. E. Weibel, and L. A. Boatner, *Phys. Rev. Lett.* **39**, 1158 (1977).
- ⁵³L. A. Boatner, U. T. Höchli, and H. E. Weibel, *Helv. Phys. Acta* **50**, 620 (1977).
- ⁵⁴U. T. Höchli, H. E. Weibel, and W. Rehwald, *J. Phys. C* **15**, 6129 (1982).
- ⁵⁵R. L. Prater, L. L. Chase, and L. A. Boatner, *Solid State Commun.* **40**, 697 (1981).
- ⁵⁶U. T. Höchli, H. E. Weibel, and L. A. Boatner, *Phys. Rev. Lett.* **41**, 1410 (1978).
- ⁵⁷J. Fousek and V. Janovek, *J. Appl. Phys.* **40**, 135 (1969).
- ⁵⁸A. P. Murani, *Solid State Commun.* **33**, 433 (1980).
- ⁵⁹B. Fischer and M. W. Klein, *Phys. Rev. Lett.* **37**, 756 (1976).
- ⁶⁰M. W. Klein, C. Held, and E. Zuroff, *Phys. Rev. B* **13**, 3576 (1976).
- ⁶¹H. Sompolinsky and A. Zippelius, *Phys. Rev. Lett.* **47**, 359 (1981).
- ⁶²H. Sompolinsky, *Phys. Rev. Lett.* **47**, 935 (1981).
- ⁶³R. C. Potter and A. C. Anderson, *Phys. Rev. B* **24**, 677 (1981).
- ⁶⁴G. D. Mahan, *Phys. Rev.* **153**, 983 (1967).
- ⁶⁵B. G. Dick, *Bull. Am. Phys. Soc.* **26**, 268 (1981).
- ⁶⁶S. H. Wemple, *Phys. Rev. B* **2**, 2679 (1970).
- ⁶⁷B. E. Vugmeister and M. D. Glinchuk, *Zh. Eksp. Teor. Fiz.* **79**, 947 (1980) [*Sov. Phys.—JETP* **52**, 3 (1980)].
- ⁶⁸W. N. Lawless, D. Rytz, and U. T. Höchli (unpublished).
- ⁶⁹R. Blinc, in *Magnetic Resonance of Phase Transitions*, edited by F. J. Owens, H. A. Farach, and C. P. Poole (Academic, New York, 1979).
- ⁷⁰Y. J. Uemura, T. Yamazaki, R. S. Hayano, R. Nakai, and C. Y. Huang, *Phys. Rev. Lett.* **45**, 583 (1980).